Mono- and Di-bridged μ-Oxo Diiron Complexes of 3-[Bis(2-pyridylmethyl)amino]propionate (bpp). Crystal Structures of $[\{Fe(bpp)(H_2O)\}_2O][ClO_4]_2\cdot H_2O$ and $[\{Fe(bpp)\}_2(MeCO_2)O][ClO_4]\cdot 4.5H_2O$†

Alan Hazell,[a] Kenneth B. Jensen,[b] Christine J. McKenzie*[,b] and Hans Toftlund[b]

[a] *Department of Chemistry, Aarhus University, DK-8000 Århus C, Denmark*

[b] *Department of Chemistry, Odense University, DK-5230 Odense M, Denmark*

Oxo-bridged dinuclear iron(III) complexes of the new tetradentate ligand, the conjugate base of 3-[bis(2-pyridylmethyl)amino]propionic acid (Hbpp), have been prepared. The structure of the monobridged μ-oxo-diiron(III) complex $[\{Fe(bpp)(H_2O)\}_2O][ClO_4]_2\cdot H_2O$ **1** shows that the bpp is co-ordinated to each iron centre as a terminal capping ligand. A water molecule completes the co-ordination sphere of each iron atom. Complex **1** crystallizes in the triclinic space group $P\bar{1}$, with $a = 13.260(4)$, $b = 14.389(4)$, $c = 11.347(3)$ Å, $\alpha = 92.224(14)$, $\beta = 113.722(13)$, $\gamma = 97.719(17)°$ and $Z = 2$. The structure refined to a final R value of 0.077 for 4249 reflections. The Fe atoms are bridged by a single μ-oxo group with average Fe–O 1.790(4) Å, Fe–O–Fe 168.8(3)° and Fe···Fe 3.564(2) Å. The cations are linked by hydrogen bonds forming chains parallel to the b axis. The co-ordinated water molecules of **1** can be replaced easily by the two co-ordinating atoms of bidentate oxo anions to form dibridged complexes. μ-Oxo complexes containing supporting μ-acetato and μ-phosphato bridges were prepared in this fashion. These substitution reactions involve a contraction of the Fe–O–Fe angle. A structural characterization of the acetato-bridged complex, $[\{Fe(bpp)\}_2(MeCO_2)O][ClO_4]\cdot 4.5H_2O$ **2**, has been carried out and shows that the iron atoms are doubly-bridged by a μ-oxide atom and μ-acetato group, with average Fe–O 1.82(2) Å, Fe–O–Fe 129(1)° and Fe···Fe 3.245(6) Å. Complexes **1** and **2** show strong antiferromagnetic coupling, as is usually observed in oxo-bridged iron pairs; $J = -114$ and -110 cm^{-1} for **1** and **2** respectively.

The last decade has witnessed an upsurge of interest in complexes incorporating oxo-bridged diiron units.[1] Much of the work in this area is motivated by their importance in understanding the chemistry of the active-site metal centres of the non-haem iron proteins such as haemerythrin, ribonuclease reductase, purple acid phosphatases and methane monooxygenase.[2]

The availability of structurally characterized model compounds containing dinuclear Fe^{II}_2 and $Fe^{II}Fe^{III}$ oxo- and hydroxo-bridged units are important if their interaction/reaction with dioxygen is to be studied.[3] So far such complexes are exceedingly rare by comparison to their Fe^{III}_2 analogues, which are somewhat less useful with regard to studies of oxygen activation. A major drawback of many of the model systems containing μ-oxo and μ-carboxylato or di-μ-carboxylato units prepared by 'spontaneous self-assembly' has been that the relatively easily synthesized diferric complexes are difficult to reduce without apparent decomposition to mononuclear iron(II) complexes.[4]

Low oxidation state diiron complexes may be stabilized by using ligands in which the potential bridging groups are anchored to the capping ligands that are useful in the synthesis of diferric model compounds. Presumably cleavage of the diiron unit becomes less likely under reducing conditions if the bridging species are connected to the terminal ligating groups. This approach has been considered with regard to the μ-oxo group. Binucleating ligands which incorporate alkoxo or phenoxo oxygen atoms, capable of bridging two iron atoms, have been used to prepare diiron(II) complexes.[5] Although these complexes have shown increased stability under reducing conditions, they prohibit the study of peroxo binding to Fe–O–Fe units, in the mode of the putative peroxo binding in oxyhaemerythrin, since the scope for hydrogen bonding to a μ-OR (R = alkyl or aryl) oxygen atom is limited. The incorporation of the potential bidentate carboxylato bridges into the ligands used for the preparation of diiron complexes has been less studied. Such ligands are somewhat more biologically relevant with regard to modelling diiron enzymes in which the carboxylate-bridging groups are derived from the protein and the μ-oxo group is derived from either dioxygen or water, and thus, not covalently bonded to a carbon atom. Beer *et al.*[6] have used the approach of linking the two μ-carboxylato ligands together in a series of diiron complexes using the bridging dicarboxylate ligand *m*-phenylenedipropionic acid. Unfortunately, extra stability, compared to the analogous monocarboxylate-bridged complexes, was not imparted to these complexes under reducing conditions.

The tripodal ligand tris(2-pyridylmethyl)amine (tpa) has been used in the preparation of μ-oxo and di-μ-oxo complexes of transition metals such as V, Cr and Mn.[7] It has proved also to be extremely useful in much of Que and co-workers work[8] in modelling the μ-oxo diiron centres in proteins. Molecular models had suggested to us that a tripodal ligand analogous to tpa but with one 2-pyridylmethyl arm replaced by an aliphatic carboxylate arm may be capable of generating structures represented by **I**. The work presented here describes our initial attempts of incorporating potential bridging-carboxylate groups into capping ligands. Binuclear iron complexes of the new tripodal ligand, the conjugate base of 3-[bis(2-pyridylmethyl)amino]propionic acid (Hbpp; $x = 2$, in **I**), are described here. Disappointingly, the arrangement in **I** was not found in the present oxo-bridged complexes. Instead bpp acts as a tetradentate tripodal ligand where the carboxylate group

† *Supplementary data available:* see Instructions for Authors, *J. Chem. Soc., Dalton Trans.*, 1993, Issue 1, pp. xxiii–xxviii.

Non-SI unit employed: G = 10^{-4} T.

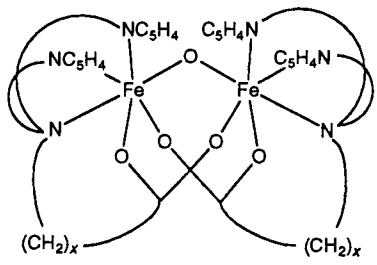

I

functions as a monodentate donor. An increase in the oxygen co-ordination around the iron atoms of diiron complexes of bpp compared to those of tpa is of interest in view of the recently reported structure of the B2 subunit of ribonuclease reductase from *Escherichia coli* (RRB2).[9] The structure displays various carboxylate co-ordinations: monodentate, Glu-238, Glu-204; bidentate, Asp-84; and bridging bidentate, Glu-115. The β-alanine-derived moiety of bpp may model some of the observed carboxylate co-ordination in RRB2.

Experimental

Infrared spectra were measured as KBr discs using a Hitachi 270-30 IR spectrometer. NMR spectra were recorded on a Bruker AC 250 FT spectrometer. UV/VIS absorption spectra were recorded on a Shimadzu UV-3100 spectrophotometer. Elemental analyses were carried out at the microanalytical laboratory of the H. C. Ørsted Institute, Copenhagen. Electron-impact mass spectra were recorded with a Varian MAT 311 A spectrometer.

CAUTION: Although no problems were encountered in the preparations of the perchlorate salts **1** and **2**, suitable care should be taken when handling such potentially hazardous compounds.

3-[*Bis*(2-*pyridylmethyl*)*amino*]*propionic Acid* (Hbpp).—Dipyridylmethylamine (3.3946 g, 17 mmol), 3-bromopropionic acid (2.5884 g, 17 mmol) and triethylamine (1.7294 g, 17 mmol) were mixed in EtOH and heated at 80 °C under dinitrogen for 18 h. On cooling, white needles of triethylamine hydrobromide separated in an approximately 80% yield. These were removed by filtration following which Hbpp together with a second crop of triethylamine hydrobromide (*ca.* 25% by weight of NEt_3HBr as judged by NMR intensities) was precipitated from the filtrate as a white crystalline solid by the addition of diethyl ether. Triethylamine hydrobromide-free Hbpp could be obtained by dissolving the solid in hot benzene (1 g in 25 cm^3), removing the undissolved triethylamine hydrobromide by filtration, and allowing the Hbpp to crystallize. Recrystallization from absolute ethanol gave Hbpp as white needles (2.64 g, 43%), m.p. 119–121 °C (Found: C, 65.90; H, 6.40; N, 15.20. $C_{15}H_{17}N_3O_2$ requires C, 66.40; H, 6.30; N, 15.50%); δ_H(250 MHz; solvent $CDCl_3$, standard $SiMe_4$) 2.62 (2 H, t, *J* 6.37, CH_2CO_2H), 3.04 (2 H, t, *J* 6.37, NCH_2CH_2), 3.95 (4 H, s, $NCH_2C_5H_4N$), 7.34–8.56 (8 H, m, C_5H_4N) and 10.77 (1 H, br s, CO_2H); δ_C(62.9 MHz; solvent $CDCl_3$, standard $SiMe_4$) 32.22 (NCH_2CH_2), 45.93 (CH_2CO_2H), 59.04 ($NCH_2C_5H_4N$), 122.42, 123.38 (C^3 and C^5 of pyridyl), 136.81 (C^4 of pyridyl), 148.70 (C^2 of pyridyl), 157.14 (C^6 of pyridyl) and 173.76 (CO_2H); ν_{max}/cm^{-1}: 1708 (OCO). Mass spectrum (electron impact): *m*/*z* 271 (M^+), 212 ($M - CH_2CO_2H$), 179 ($M - CH_2C_5H_4N$), 135 ($M - CH_2C_5H_4N - CH_2CO_2H$), 93 ($CH_2C_5H_4NH$) and 92 ($CH_2C_5H_4N$).

Bis(*aqua*)*bis*{3-[*bis*(2-*pyridylmethyl*)*amino*]-*propionato*}-μ-*oxo-diiron*(III) *Perchlorate* $[\{Fe(bpp)(H_2O)\}_2O][ClO_4]_2$ **1**.—A mixture of Hbpp (1.039 g, 3.8 mmol) and triethylamine (0.382 g, 3.8 mmol) dissolved in methanol–water (1 : 1, 10 cm^3) was added to a solution of $Fe(ClO_4)_3 \cdot 6H_2O$ (1.899 g, 4.1 mmol) in methanol (5 cm^3). The solution changed to deep red within seconds. On standing, dark red cubic-shaped crystals were deposited. The product was filtered off, washed with methanol and dried in vacuum (1.340 g, 78%) {Found: C, 37.90; H, 4.15; Cl, 7.70; N, 8.85. $[\{Fe(bpp)(H_2O)\}_2O][ClO_4]_2 \cdot 4H_2O$, $C_{30}H_{40}Cl_2Fe_2N_6O_{19}$ requires C, 38.35; H, 4.30; Cl, 7.55; N, 8.95%}.

μ-*Acetato-bis*{3-[*bis*(2-*pyridylmethyl*)*amino*]*propionato*}-μ-*oxo-diiron*(III) *Perchlorate* $[\{Fe(bpp)\}_2(MeCO_2)O][ClO_4]$ **2**.—Sodium acetate trihydrate (2.412 g, 17.7 mmol) dissolved in water (10 cm^3) was added to a suspension of $[\{Fe(bpp)(H_2O)\}_2O][ClO_4]_2 \cdot 4H_2O$ (1.90 g, 2.02 mmol) in methanol (30 cm^3). The complex slowly dissolved on heating to give a deep green solution. The solvent was removed under reduced pressure and the residue dissolved in water (1 cm^3). Emerald green octahedral crystals were deposited on standing. These were collected, washed with cold methanol and dried in vacuum (0.0456 g, 47%) {Found: C, 41.45; H, 4.40; Cl, 3.32; N, 9.05. $[\{Fe(bpp)\}_2(MeCO_2)O][ClO_4] \cdot 5H_2O$, $C_{32}H_{45}ClFe_2N_6O_{16}$ requires C, 41.90; H, 4.95; Cl, 3.85; N, 9.15%}.

Bis{3-[*bis*(2-*pyridylmethyl*)-*amino*]*propionato*}(μ-*diphenylphosphato*)-μ-*oxo-diiron*(III) *Perchlorate*, $[\{Fe(bpp)\}_2\{O_2P(OPh)_2\}O][ClO_4]$ **3** *and Bis*{3-[*bis*(2-*pyridylmethyl*)*amino*]-*propionato*}-μ-*oxo*-μ-*phenylphosphato-diiron*(III) $[\{Fe(bpp)\}_2\{O_3P(OPh)\}O]$ **4**.—The phosphato-bridged complexes were prepared *in situ* by mixing approximately 1 equivalent of the sodium salts of diphenylphosphate and phenylphosphate with the diaqua complex **1** dissolved in acetonitrile–water (1 : 1). A colour change from red to the characteristic green colour of the dibridged complexes was observed. Reaction solvents and counter anions were varied, however we were unable to induce the precipitation of these phosphato-bridged complexes.

Resonance Raman Studies.—Raman spectra were recorded on a Jarrell-Ash, Czerny-Turner scanning spectrometer. The samples were prepared as discs containing 300 mg of KBr, 20 mg of the complex and 20 mg of K_2SO_4 for use as internal standard [referenced to $\nu_1(SO_4^{2-})$]. The spectra of each sample were recorded at three excitation wavelengths, 457.9, 487.9 and 514.5 nm.

Magnetic Studies.—Magnetic susceptibility measurements using the Faraday method were carried out on solid samples of complexes **1** and **2** in the temperature range 4–300 K at a field strength of 1.3 T using instrumentation described elsewhere.[10] The variation of susceptibility with temperature can be described by the equation derived from the Heisenberg, Dirac, van Vleck model for isotropic dinuclear magnetic exchange interactions ($H = -2JS_1 \cdot S_2$).[11] The molar susceptibility was corrected for underlying ligand diamagnetism by the use of Pascal's constants and fitted by a least-square method to equation (1) where $x = J/kT$, p = mole fraction of paramagnetic impurities and t.i.p. = temperature-independent paramagnetism.

Electron Spin Resonance.—ESR spectra were recorded in the temperature range 200–306 K on a Bruker ESP 300 spectrometer operating at a frequency of 9.38 GHz (X-band) with magnetic-field modulation of 100 kHz, modulation amplitude of 5 G and microwave power of 10 mW. Samples were examined in the solid state as neat powders.

$$\chi_M = (1 - p)\left\{\frac{Ng^2\mu_B^2}{kT}\right\}\left\{\frac{2e^{2x} + 10e^{6x} + 28e^{12x} + 60e^{20x} + 110e^{80x}}{1 + 3e^{2x} + 5e^{6x} + 7e^{12x} + 9e^{20x} + 11e^{30x}}\right\} + \frac{p35}{8T} + \text{t.i.p.} \quad (1)$$

X-Ray Crystallography.—Crystals of **1** suitable for X-ray diffraction studies were grown by slow evaporation of the filtrate after the isolation of the first crop of the complex. Crystals of **2** suitable for X-ray studies were obtained directly from the reaction mixture.

Cell dimensions were determined from reflections measured at four positions, $\pm 2\theta$ and high and low χ. Intensities were measured at room temperature using a Huber diffractometer. The intensities of two standard reflections were measured every 50 reflections. Crystal data for complexes **1** and **2** are given in Table 1.

Data were corrected for background, Lorentz and polarization effects and for absorption. The structures were determined using SHELX 86[12] and from subsequent difference electron density maps and were refined by the least-squares minimization of $\Sigma w(|F_o| - |F_c|)^2$ using a modification of ORFLS.[13] For complex **1**, atoms C(1) and C(2) were found to be disordered, the occupation factors were constrained to be the same for C(1) and C(2), occupancy = 0.549(29), and for C(1′) and C(2′), occupancy = 1 − 0.549(29). All hydrogen atoms were located on a difference map except for those on the disordered atoms. All non-hydrogen atoms, except C(1) and C(1′) were refined with anisotropic thermal parameters. Hydrogen atoms were kept fixed at calculated positions except for those on the oxygen atoms, a common isotropic thermal parameter was refined for the hydrogen atoms. Fractional atomic coordinates for complex **1** are listed in Table 2. The crystals of complex **2** were found to be very weakly diffracting, and consequently, there are an insufficient number of significant reflections to warrant anisotropic refinement for atoms other than Fe and Cl. The hydrogen atoms of the ligands were kept in calculated positions. Although the structure obtained for complex **2** is of low accuracy, it is essentially correct. Fractional atomic coordinates for complex **2** are listed in Table 3.

Additional material available from the Cambridge Crystallographic Data Centre comprises H-atom coordinates, thermal parameters and remaining bond lengths and angles.

Table 1 Structure analysis for $[\{Fe(bpp)(H_2O)\}_2O][ClO_4]_2\cdot H_2O$ **1** and $[\{Fe(bpp)\}_2(MeCO_2)O][ClO_4]\cdot 4.5H_2O$ **2**

	1	**2**
Formula	$C_{30}H_{38}Cl_2Fe_2N_6O_{16}$	$C_{32}H_{44}ClFe_2N_6O_{15.5}$
M	921.2	907.9
Crystal system	Triclinic	Monoclinic
Space group	$P\bar{1}$	$P2_1/a$
a/Å	13.260(4)	22.845(7)
b/Å	14.389(4)	15.573(3)
c/Å	11.347(3)	23.310(4)
α/°	92.224(14)	90.0
β/°	113.722(13)	90.944(15)
γ/°	97.719(17)	90.0
U/Å^3	1954(1)	8292(3)
Z	2	8
D_c/g cm^{-3}	1.566	1.454
$F(000)$	948	3768
μ(Mo-Kα)/cm^{-1}	9.46	8.33
Crystal dimensions/mm	0.6 × 0.5 × 0.4	0.3 × 0.3 × 0.6
Scan type	ω–2θ	ω
2θ Range/°	2–50	2–40
Steps per scan	50	40
ω Scan width/°	1.4 + 0.346tanθ	1.8 + 0.346tanθ
No. of unique data	6906	7758
No. of data with $I/\sigma(I) > 3.0$	4249	2244
No. of variables	534	485
Systematic absences	—	$h0l$ with h odd $0k0$ with k odd
R	0.077	0.085
R'	0.092	0.107

Table 2 Fractional coordinates for $[\{Fe(bpp)(H_2O)\}_2O][ClO_4]_2\cdot H_2O$ **1**

Atom	x	y	z	Atom	x	y	z
Fe(1)	0.8658(1)	0.8356(1)	0.2459(1)	C(25)	0.5399(7)	0.6660(8)	0.1306(10)
Fe(2)	1.0843(1)	0.7016(1)	0.3883(1)	C(26)	0.6281(7)	0.7365(6)	0.1532(8)
O(2)	0.9449(4)	0.9681(4)	0.3092(5)	C(27)	0.6174(7)	0.8386(7)	0.1486(8)
O(3)	0.8331(5)	0.8512(5)	0.4117(6)	C(32)	1.2092(7)	0.9073(6)	0.4205(8)
O(4)	0.9786(4)	0.7700(4)	0.3040(5)	C(33)	1.2950(8)	0.9824(6)	0.4679(9)
O(6)	0.9982(4)	0.5767(4)	0.3762(5)	C(34)	1.3970(8)	0.9639(7)	0.5577(9)
O(7)	1.0903(5)	0.7232(4)	0.5725(6)	C(35)	1.4084(7)	0.8756(7)	0.5929(9)
N(1)	0.7083(5)	0.8899(4)	0.1243(6)	C(36)	1.3195(7)	0.8037(6)	0.5437(8)
N(2)	1.2424(5)	0.6396(5)	0.4697(6)	C(37)	1.3223(7)	0.7055(7)	0.5786(9)
N(11)	0.8799(5)	0.8563(4)	0.0665(6)	C(42)	1.0242(8)	0.6498(6)	0.0974(9)
N(21)	0.7336(5)	0.7169(5)	0.1882(6)	C(43)	1.0376(9)	0.6187(7)	−0.0119(9)
N(31)	1.2188(5)	0.8202(5)	0.4522(6)	C(44)	1.1370(11)	0.5904(8)	0.0056(10)
N(41)	1.1036(6)	0.6526(5)	0.2172(6)	C(45)	1.2193(9)	0.5903(7)	0.1299(10)
C(1)	0.7207(12)	0.9971(11)	0.1263(19)	C(46)	1.2010(7)	0.6230(6)	0.2336(8)
C(1′)	0.7078(18)	0.9893(15)	0.1775(26)	C(47)	1.2869(7)	0.6309(6)	0.3693(9)
C(2)	0.7832(12)	1.0418(10)	0.2671(20)	C(11)	0.3436(2)	0.8560(2)	−0.8380(2)
C(2′)	0.8059(20)	1.0542(14)	0.1905(28)	O(11)	0.4143(6)	0.8110(5)	−0.7334(7)
C(3)	0.9119(7)	1.0445(6)	0.3134(8)	O(12)	0.3982(7)	0.9490(6)	−0.8265(8)
O(1)	0.9739(5)	1.1175(4)	0.3769(6)	O(13)	0.3316(7)	0.8110(6)	−0.9573(8)
C(4)	1.2220(7)	0.5467(7)	0.5151(9)	O(14)	0.2369(6)	0.8522(7)	−0.8382(10)
C(5)	1.1352(8)	0.4725(6)	0.4158(9)	C(12)	0.6470(3)	0.6366(2)	0.7583(3)
C(6)	1.0154(7)	0.4920(6)	0.3627(8)	O(21)	0.6031(8)	0.7163(7)	0.7196(11)
O(5)	0.9380(5)	0.4251(4)	0.3107(6)	O(22)	0.6839(21)	0.6336(11)	0.8892(14)
C(12)	0.9763(7)	0.8583(6)	0.0507(9)	O(23)	0.5810(11)	0.5517(8)	0.7029(13)
C(13)	0.9829(8)	0.8762(7)	−0.0638(10)	O(24)	0.7427(13)	0.6407(11)	0.7448(23)
C(14)	0.8935(9)	0.8977(8)	−0.1640(9)	O(25)	0.6755(22)	0.7474(24)	0.4740(31)
C(15)	0.7948(8)	0.8983(7)	−0.1488(9)	H(O3A)	0.881(7)	0.864(6)	0.492(9)
C(16)	0.7899(6)	0.8775(6)	−0.0358(8)	H(O3B)	0.792(8)	0.811(6)	0.425(8)
C(17)	0.6846(7)	0.8682(6)	−0.0140(8)	H(O7A)	1.076(8)	0.771(6)	0.584(9)
C(22)	0.7511(7)	0.6277(6)	0.1961(8)	H(O7B)	1.064(7)	0.678(6)	0.599(8)
C(23)	0.6642(9)	0.5549(6)	0.1737(9)	H(O25A)	0.636(16)	0.784(14)	0.444(23)
C(24)	0.5564(8)	0.5767(8)	0.1378(10)	H(O25B)	0.720(9)	0.729(8)	0.546(10)

Table 3 Fractional atomic coordinates for $[\{Fe(bpp)\}_2(MeCO_2)O][ClO_4]\cdot 4.5H_2O$ **2**

	Cation 1			Cation 2		
Atom	*x*	*y*	*z*	*x*	*y*	*z*
Fe(1)	0.6366(3)	0.0567(3)	0.3604(2)	0.4051(3)	0.1797(4)	0.1064(2)
Fe(2)	0.6029(2)	0.2589(3)	0.3606(2)	0.3727(2)	−0.0214(4)	0.1249(2)
O(1)	0.6287(9)	0.1627(13)	0.3924(7)	0.3736(10)	0.0760(13)	0.0860(8)
O(2)	0.6060(10)	0.0813(14)	0.2798(8)	0.4470(12)	0.1396(17)	0.1809(10)
O(3)	0.7174(11)	0.0617(15)	0.3315(8)	0.3977(10)	0.0228(15)	0.2044(8)
O(4)	0.8070(13)	0.0176(19)	0.3360(10)	0.4784(12)	0.1827(18)	0.0627(10)
O(5)	0.5999(9)	0.2242(14)	0.2758(8)	0.5164(14)	0.2437(21)	−0.0111(14)
O(6)	0.5179(11)	0.2454(16)	0.3669(8)	0.2914(11)	−0.0221(17)	0.1515(9)
O(7)	0.4323(14)	0.2640(19)	0.3952(11)	0.2026(14)	−0.0613(17)	0.1823(10)
N(11)	0.6329(15)	−0.0847(18)	0.3338(12)	0.4323(15)	0.3133(19)	0.1334(12)
N(12)	0.6740(11)	−0.0067(21)	0.4352(9)	0.3678(13)	0.2571(20)	0.0386(11)
N(13)	0.5508(12)	0.0093(21)	0.3817(11)	0.3359(13)	0.2228(18)	0.1600(11)
N(31)	0.5856(13)	0.3961(17)	0.3322(11)	0.3867(14)	−0.1555(19)	0.1636(11)
N(32)	0.6002(12)	0.3318(19)	0.4401(11)	0.3473(13)	−0.1021(19)	0.0566(12)
N(33)	0.6859(12)	0.3149(17)	0.3418(10)	0.4672(13)	−0.0530(19)	0.1144(12)
C(1)	0.5997(16)	0.1517(27)	0.2537(14)	0.4296(18)	0.0850(26)	0.2134(16)
C(2)	0.5981(15)	0.1415(22)	0.1875(13)	0.4485(18)	0.0964(24)	0.2800(16)
C(11)	0.6509(16)	−0.1387(24)	0.3835(14)	0.3977(19)	0.3807(27)	0.0973(18)
C(12)	0.6783(17)	−0.0918(24)	0.4297(14)	0.3772(18)	0.3393(28)	0.0417(16)
C(13)	0.7179(19)	−0.1338(25)	0.4677(17)	0.3647(21)	0.3978(29)	−0.0038(20)
C(14)	0.7457(18)	−0.0822(26)	0.5116(16)	0.3423(20)	0.3518(32)	−0.0536(18)
C(15)	0.7387(15)	0.0011(32)	0.5190(13)	0.3324(16)	0.2680(26)	−0.0584(15)
C(16)	0.6991(16)	0.0347(22)	0.4764(15)	0.3452(16)	0.2225(22)	−0.0095(15)
C(21)	0.5724(19)	−0.0959(23)	0.3162(16)	0.4054(17)	0.3213(23)	0.1935(14)
C(22)	0.5329(21)	−0.0618(29)	0.3573(17)	0.3478(17)	0.2876(22)	0.1942(14)
C(23)	0.4833(23)	−0.0977(28)	0.3666(18)	0.3034(19)	0.3198(24)	0.2279(14)
C(24)	0.4479(20)	−0.0578(31)	0.4033(19)	0.2496(19)	0.2883(25)	0.2259(15)
C(25)	0.4621(19)	0.0191(28)	0.4324(15)	0.2344(16)	0.2008(22)	0.1908(14)
C(26)	0.5149(20)	0.0441(23)	0.4168(16)	0.2814(18)	0.1876(23)	0.1583(14)
C(27)	0.7594(18)	0.0069(29)	0.3229(13)	0.5070(19)	0.2484(33)	0.0430(18)
C(28)	0.7412(19)	−0.0815(25)	0.3049(15)	0.5199(19)	0.3218(29)	0.0758(18)
C(29)	0.6764(20)	−0.0936(25)	0.2892(17)	0.4952(20)	0.3210(27)	0.1317(17)
C(31)	0.5924(15)	0.4585(21)	0.3826(13)	0.3840(17)	−0.2216(25)	0.1158(15)
C(32)	0.5919(17)	0.4140(25)	0.4398(16)	0.3494(15)	−0.1895(24)	0.0629(13)
C(33)	0.5851(15)	0.4624(22)	0.4894(16)	0.3325(18)	−0.2506(27)	0.0220(16)
C(34)	0.5897(21)	0.4217(31)	0.5401(19)	0.3074(19)	−0.2187(28)	−0.0284(17)
C(35)	0.6017(21)	0.3330(34)	0.5425(19)	0.3018(18)	−0.1326(28)	−0.0362(16)
C(36)	0.6050(19)	0.2877(26)	0.4899(18)	0.3238(19)	−0.0688(27)	0.0066(17)
C(41)	0.6290(18)	0.4143(22)	0.2886(15)	0.4465(17)	−0.1553(24)	0.1900(14)
C(42)	0.6876(20)	0.3911(26)	0.3091(16)	0.4867(18)	−0.1139(23)	0.1511(14)
C(43)	0.7394(22)	0.4310(26)	0.2974(16)	0.5471(20)	−0.1324(25)	0.1497(16)
C(44)	0.7884(22)	0.4034(29)	0.3185(18)	0.5826(21)	−0.0838(30)	0.1129(19)
C(45)	0.7912(20)	0.3229(30)	0.3514(17)	0.5591(19)	−0.0246(28)	0.0768(15)
C(46)	0.7385(19)	0.2821(24)	0.3588(14)	0.4995(17)	−0.0107(29)	0.0766(14)
C(47)	0.4784(21)	0.2926(29)	0.3690(16)	0.2544(23)	−0.0761(26)	0.1728(16)
C(48)	0.4775(18)	0.3787(26)	0.3460(16)	0.2822(19)	−0.1698(27)	0.1859(15)
C(49)	0.5253(18)	0.3995(23)	0.3065(15)	0.3403(19)	−0.1726(25)	0.2069(15)
Anions and solvent of crystallization *						
Cl(1)	0.2691(8)	0.5608(9)	0.1273(6)	O(23)	−0.1663(14)	0.1391(20)	0.4276(12)
Cl(2)	0.7114(12)	0.1702(11)	0.6376(6)	O(24)	−0.1520(18)	0.1549(27)	−0.4549(16)
O(15)	0.3170(37)	0.5705(51)	0.1344(33)	O(25)	0.1325(19)	0.0600(26)	0.1410(16)
O(16)	0.2476(16)	0.4922(33)	0.1572(15)	O(26)	0.0981(19)	0.0876(26)	−0.3055(17)
O(17)	0.2425(20)	0.5651(27)	0.0746(19)	O(27)	0.0801(24)	0.0636(32)	−0.1964(21)
O(18)	0.2438(19)	0.6301(30)	0.1540(17)	O(28)	−0.0350(25)	0.0608(34)	−0.1552(22)
O(19)	0.7635(33)	0.1865(49)	0.6623(30)	O(29)	0.0282(32)	0.0802(42)	−0.0533(27)
O(20)	0.6861(29)	0.2387(47)	0.6633(26)	O(31)	0.4509(27)	0.2240(41)	−0.4862(23)
O(21)	0.7047(15)	0.1778(23)	0.5819(16)	O(32)	−0.1086(30)	0.1696(45)	−0.2223(27)
O(22)	0.6855(15)	0.1014(23)	0.6551(13)			

* O(15)–O(18) Perchlorate oxygen atoms attached to Cl(1), O(19)–O(22) perchlorate oxygen atoms attached to Cl(2), O(23)–O(32) water molecules.

Results and Discussion

The reaction of 3-[bis(2-pyridylmethyl)amino]propionic acid (Hbpp) and iron(III) perchlorate in methanol–water in the absence of other potential ligands gives, instead of the structure represented by **I**, the diaqua complex, $[\{Fe(bpp)(H_2O)\}_2O][ClO_4]_2$ **1**. The X-ray crystal structure of **1**, see below, shows a *cis* arrangement for the water molecules attached to each iron atom of the nearly linear Fe–O–Fe core. The water ligands of complex **1** proved to be extremely labile and are geometrically suitably positioned to undergo substitution reactions. In order to explore the chemistry of μ-oxo-diiron(III) centres relevant to their functions in biology, it is desirable to isolate complexes such as **1** in which one or more co-ordination sites are available for ligand substitution. Complex **1** proved to be a suitable starting material for the synthesis of several dibridged complexes; the *cis* water ligands are easily substituted for mono-

Table 4 Spectroscopic and magnetic properties of $[\{Fe(bpp)\}_2(X)O][ClO_4]_n$ complexes

X	$(H_2O)_2$ **1**	$MeCO_2^-$ **2**	$O_2P(OPh)_2^-$ **3**[a]	$O_3P(OPh)^{2-}$ **4**[a]	$PhCO_2$ **5**[a,b]
Electronic spectra[c]					
λ_{max}/nm	326 (11 910)	329 (10 230)	317 (10 674)	312 (10 373)	328 (7400)
(ε/dm^3 mol^{-1} cm^{-1})	353 (10 350)	353 (sh) (8720)	353 (8302)	347 (8103)	360 (sh)
	412 (1840)	413 (1710)	408 (sh) (1535)		410 (sh)
	475 (sh) (320)	441 (sh) (974)		440 (574)	
	486 (370)	488 (653)	478 (402)	487 (299)	488 (600)
	515 (180)	520 (240)	508 (186)	508 (sh) (155)	510 (sh)
	570 (180)	626 (170)	595 (163)	584 (119)	632 (200)
IR and resonance Raman spectra					
ν_{asym}, ν_{sym} (Fe–O–Fe)/cm^{-1}[d]	822, 379	767, 495			
Magnetic properties					
$-J$/cm^{-1}	114	110			
t.i.p./cm^3 mol^{-1}	0.000 280	0.000 090			
p	0.0090	0.0017			
g	2.06	1.93			

[a] Characterized only in solution. [b] Data taken from ref. 14. [c] Complex **1** in dimethylformamide, complexes **2**–**4** in MeCN–H_2O (1 : 1), complex **5** in methanol. [d] ν_{asym} from IR spectrum; ν_{sym} from resonance Raman spectrum.

anionic acetate and diphenylphosphate to give $[\{Fe(bpp)\}_2(MeCO_2)O][ClO_4]$ **2** and $[\{Fe(bpp)\}_2\{O_2P(OPh)_2\}O][ClO_4]$ **3** and dianionic phenylphosphate to give $[\{Fe(bpp)\}_2\{O_3P(OPh)\}O]$ **4**. Some physical properties of these complexes are listed in Table 4. The X-ray crystal structure of **2**, has been determined, see below.

During the course of the present work the benzoate-bridged complex homologue to **2**, $[\{Fe(bpp)\}_2(PhCO_2)O][ClO_4]$ **5**, was characterized from its spectral properties in solutions.[14] The UV/VIS data for this complex are listed also in Table 4. The similarities of the UV/VIS spectrum of the carboxylato-bridged complex structurally characterized in the present work, **2**, and that reported for **5**, indicate similar core structures and supports the assignment of **5**. Apparently the isolation of **5** in the solid state proved difficult.[14] This is consistent with our experience of the complexes of bpp described here. Often a period of several weeks was required for the crystallization of complex **2**. The growth of crystals appeared also to be very sensitive to solvent composition (methanol : water ratio). We did not succeed in the isolation of the phosphato-bridged complexes **3** and **4** in the solid state, however, based on solution spectral properties, we can be reasonably certain of the assignment of dibridged μ-oxo-μ-phosphato core structures.

The UV/VIS spectra of the bpp complexes (Table 4) show a general blue shift of the bands characteristic of μ-oxo Fe^{III}_2 complexes compared to the previously reported tpa analogues. The replacement of one 2-pyridylmethyl group by an aliphatic carboxylate reflects the relative positions of these donor groups in the spectrochemical series. The observed blue shift supports an assignment of the low energy features to ligand-field transitions, since the energy of the two first transitions, $^6A_1 \longrightarrow {}^4T_2$, $^6A_1 \longrightarrow {}^4T_1$, are both expected to decrease with increasing Δ. Replacing pyridine for carboxylate might also induce a blue shift of a ligand-to-metal charge-transfer (l.m.c.t.) transition, since a negatively charged ligand will stabilize the high oxidation state of the metal centres and thereby lower their optical electronegativity. Thus, the position of the characteristic band in the region 550–800 cm^{-1} of the UV/VIS spectrum for **2** at 626 nm is closer to the corresponding feature reported for RRB2 at 600 nm ($\varepsilon_{mmol\,dm^{-3}}$ 0.15)[15] than is the band at 700 nm reported for $[\{Fe(tpa)\}_2(MeCO_2)O][ClO_4]_3$.[8c] The band in the region 550–800 cm^{-1} of the spectra of the multiply-bridged μ-oxo-diiron(III) complexes has been observed also to blue-shift with increasing bite angle of the supporting bridge and consequent expansion of the Fe–O–Fe angle. This phenomenon was examined by Que and co-workers[8d] in the series of tpa complexes in which the supporting bridge was systematically varied in order to study the effect of the Fe–O–Fe angle on physical properties. A blue shift of this band in the complexes of bpp, parallel to that observed with the tpa complexes, is evident, on going from the carboxylate-bridged complexes **2** and **5** (626 and 632 nm respectively), to the phosphato-bridged complexes **3** and **4** (595 and 584 nm respectively), and finally to the almost linear diaqua complex **1**, where it appears as a shoulder at 570 nm in aqueous solution. Complex **1** gives a better defined spectrum in the potentially co-ordinating solvents acetonitrile and dimethylformamide where the water ligands are probably replaced by solvent molecules. It has been shown that the Fe–O–Fe angle in μ-oxo-diiron complexes is a more important factor, than the nature of the terminal ligands, in the determination of the spectral features. Thus, the exchange of the terminal water molecules for other solvent molecules is not expected to significantly alter the geometry, and hence, the spectral features of the complexes.

The Raman spectra of **1** and **2** (Table 4) are typical of oxo-bridged species. The dominant feature is the symmetric stretching mode, ν_{sym}(Fe–O–Fe) at 379 cm^{-1} for **1** and 495 cm^{-1} for **2**. These values fall into the ranges recorded previously for a series of monobridged (363–425 cm^{-1}) and dibridged (454–499 cm^{-1}) diiron complexes.[16] The band at 495 cm^{-1} recorded for **2** is very close to the Raman feature at 493 cm^{-1} assigned to ν_{sym}(Fe–O–Fe) for RRB2.[17] The ν_{sym}(Fe–O–Fe) for $[\{Fe(tpa)\}_2(MeCO_2)O][ClO_4]$ was observed at 499 cm^{-1}.[16] Since these values are extremely close, it can be concluded, that the terminal ligation in the three systems has not affected the vibrational mode of the Fe(μ-O)(μ-RCO_2)Fe unit to any significant extent.

The J values of −114 and −110 cm^{-1} obtained for complexes **1** and **2** are similar and imply strong antiferromagnetic coupling. The strength of the antiferromagnetic coupling is not significantly affected by either the differences in the Fe–O–Fe angle or by the presence of the acetato bridge in **2**.

At ambient temperature complex **2** gives a complicated ESR spectrum with several broad features in the range 225–5000 G at X-band frequency. The intensities of several of these features change markedly with temperature, and at 200 K no resolvable bands are apparent. The transitions arising from within a given spin multiplet (*i.e.* $\Delta S = 0$) change in intensity according to the Boltzmann population of the levels of the multiplet and can be used to estimate the energy of the multiplet with reference to the ground state according to equation (2), where ΔE = transition-energy difference, E = multiplet energy and I = intensity of

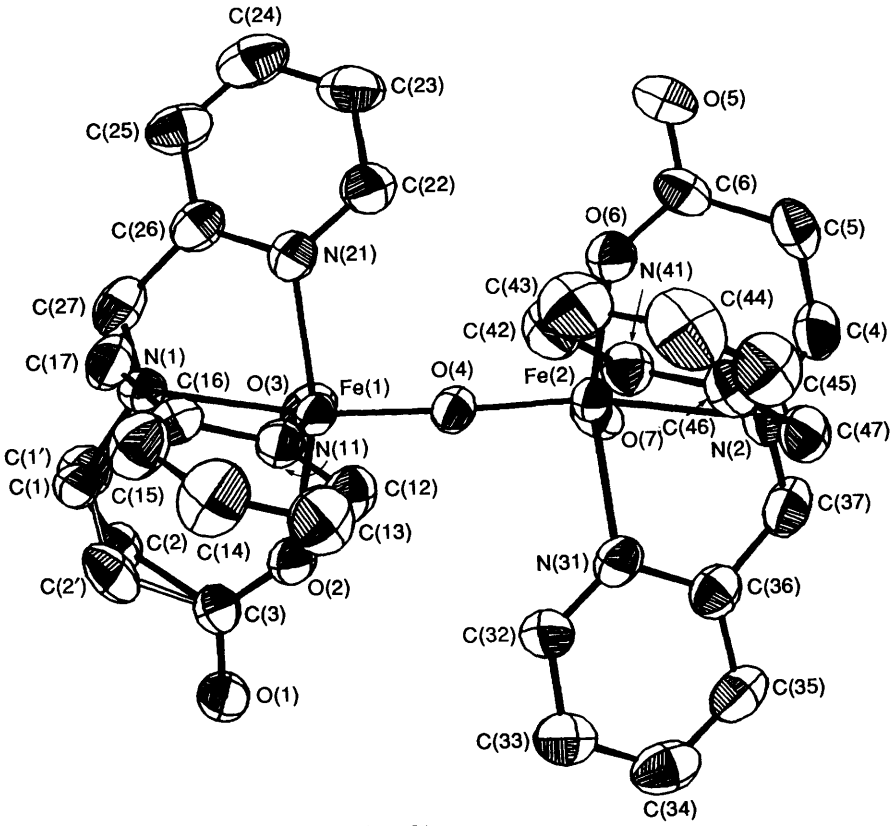

Fig. 1 The molecular geometry of the cation $[\{Fe(bpp)(H_2O)\}_2O]^{2+}$ in **1**. The two sets of positions for the methylene carbon atoms of the disordered chelate ring are shown. The bonds to C(1) and C(2) are filled and those to C(1') and C(2') are unfilled

transition. Equation (2) leads to relation (3) where a is a constant when $\Delta E \ll kT$.

$$I \propto \exp\left(\frac{-E}{kT}\right) - \exp\left\{\frac{-(E + \Delta E)}{kT}\right\} \quad (2)$$

$$\ln (IT) = a - (E/kT) \quad (3)$$

The spectrum of **2** was recorded at 265, 275, 300 and 306 K. The double integration of the first derivative spectrum gives the intensity of the three best resolved bands, occurring at g values of 11, 5 and 3.7. The multiplet energies were estimated from the intensity *vs.* T variations to be 1109, 1337 and 693 cm^{-1} respectively. The comparison of these energies with the J values calculated from the susceptibility measurements suggests that the two first transitions are occurring within the $S = 3$ multiplet, $12J$ above the ground state and the third within the $S = 2$ multiplet, $6J$ above the ground state. This gives J values of 92, 111 and 115 cm^{-1}, respectively. These values are reasonably well in accordance with the $J = 110$ cm^{-1} obtained from the fit of the magnetic susceptibility.

Crystal and Molecular Structure of $[\{Fe(bpp)(H_2O)\}_2O][ClO_4]_2 \cdot H_2O$ **1**.—The cation in complex **1** is shown in Fig. 1. The geometry around the iron atoms is approximately octahedral. Each iron atom is co-ordinated to the three nitrogen atoms and a carboxylate oxygen atom of the bpp, the bridging oxygen atom and a water molecule. The Fe ··· Fe separation of 3.564(2) Å, the Fe–O–Fe angle of 168.8(3)° and average Fe–μ-O of 1.790(4) Å, are typical values for oxo-bridged diiron complexes. Important interatomic distances and angles are given in Table 5. The oxygen atoms of the water ligands attached to Fe(1) and Fe(2), O(3) and O(7), respectively, are positioned *cis* to each other. The carboxylate oxygen donor atoms of each bpp ligand, O(6) and O(2), are located *trans* to each other. The $Fe–O_{aqua}$ distances [av. 2.086(7) Å] are longer than the $Fe–O_{carboxylate}$ distances [av. 1.983(6) Å]. The μ-oxo group is expected to have a strong *trans* influence hence the weakest donor atom of bpp, the tertiary amine nitrogen, is located *trans* to this group. The $Fe–N_{amine}$ bonds *trans* to the oxo bridge are longer [av. 2.251(6) Å] than the $Fe–N_{pyridine}$ bonds *cis* to the bridge [av. 2.153(7) Å]. The cation is linked by hydrogen bonds to its neighbour at $2 - x$, $1 - y$, $1 - z$, $O(3) \cdots O(1^i) = 2.678(8)$ Å and $O(7) \cdots O(1^i) = 2.669(8)$ Å, thus forming chains parallel to the b axis. The water of crystallization is hydrogen bonded to O(3), $O(25) \cdots O(3) = 2.75(3)$ Å.

Table 5 Selected bond distances (Å) and angles (°) for $[\{Fe(bpp)(H_2O)\}_2O][ClO_4]_2 \cdot H_2O$ **1**

Fe(1) ··· Fe(2)	3.564(2)	Fe(2)–O(4)	1.792(5)
Fe(1)–O(4)	1.788(5)	Fe(2)–O(6)	1.965(6)
Fe(1)–O(2)	2.000(5)	Fe(2)–O(7)	2.069(7)
Fe(1)–O(3)	2.103(6)	Fe(2)–N(2)	2.247(6)
Fe(1)–N(1)	2.254(6)	Fe(2)–N(41)	2.162(7)
Fe(1)–N(11)	2.146(6)	Fe(2)–N(31)	2.159(7)
Fe(1)–N(21)	2.145(7)		
O(4)–Fe(1)–O(2)	101.9(2)	O(4)–Fe(2)–O(6)	103.1(2)
O(4)–Fe(1)–O(3)	100.3(2)	O(4)–Fe(2)–O(7)	99.6(2)
O(4)–Fe(1)–N(21)	96.6(3)	O(4)–Fe(2)–N(31)	94.5(3)
O(4)–Fe(1)–N(11)	94.3(2)	O(4)–Fe(2)–N(41)	94.6(2)
O(4)–Fe(1)–N(1)	164.3(2)	O(4)–Fe(2)–N(2)	164.7(2)
O(2)–Fe(1)–O(3)	81.9(2)	O(6)–Fe(2)–O(7)	86.6(2)
O(2)–Fe(1)–N(21)	158.6(2)	O(6)–Fe(2)–N(31)	161.4(2)
O(2)–Fe(1)–N(11)	87.8(2)	O(6)–Fe(2)–N(41)	87.6(2)
O(2)–Fe(1)–N(1)	90.0(2)	O(6)–Fe(2)–N(2)	89.3(2)
O(3)–Fe(1)–N(21)	84.4(3)	O(7)–Fe(2)–N(31)	84.6(3)
O(3)–Fe(1)–N(11)	163.6(3)	O(7)–Fe(2)–N(41)	165.6(2)
O(3)–Fe(1)–N(1)	91.4(2)	O(7)–Fe(2)–N(2)	89.9(2)
N(21)–Fe(1)–N(11)	101.4(2)	N(31)–Fe(2)–N(41)	97.1(2)
N(21)–Fe(1)–N(1)	73.9(2)	N(31)–Fe(2)–N(2)	74.4(3)
N(11)–Fe(1)–N(1)	75.8(2)	N(41)–Fe(2)–N(2)	76.9(2)
Fe(1)–O(4)–Fe(2)	168.8(3)		

Crystal and Molecular Structure of $[\{Fe(bpp)\}_2(MeCO_2)O][ClO_4]\cdot 4.5H_2O$ **2**.—The crystal structure contains two crystallographically unique but chemically identical $[\{Fe(bpp)\}_2(MeCO_2)O]^+$ units, together with perchlorate anions and solvent water molecules. The geometries for the cations are similar but not identical. The atomic arrangement for cation 2 together with the numbering scheme used for both cations is shown in Fig. 2. Selected interatomic distances and bond angles are given in Table 6. The iron atoms, doubly-bridged by the μ-oxo and μ-acetato groups, are each co-ordinated to the three nitrogen atoms and a carboxylate oxygen atom of the bpp, the bridging oxygen atom and an oxygen of the bridging acetate group in an approximately octahedral arrangement. The geometrical arrangement is related to that shown for **1**, with the co-ordinated carboxylato-oxygen donor atoms of the bpp located *trans* to each other, relative to the plane passing through the bridging acetato and oxo groups. The tertiary amine donors of the bpp, again, are both located *trans* to the μ-oxo group. The $Fe–N_{amine}$ bonds [av. 2.28(3) Å] *trans* to the oxide bridge are longer than the $Fe–N_{pyridine}$ bonds [2.16(3) Å] *cis* to the bridge. The interatomic distances, Fe(1)···Fe(2), of 3.241(7) Å for cation 1 and 3.249(9) Å for cation 2 [av. 3.245(6) Å] and Fe–O–Fe angles of 129(1)°, are, as expected, considerably less than the analogous values for complex **1**.

The symmetrical arrangements observed in the solid-state structures of both complex **1** and **2**, in which the tertiary amine donors of the bpp are both *trans* to the oxo bridge, can be contrasted to the asymmetric structures observed in the dibridged diiron complexes of tpa reported by Que and co-workers.[8c,d] Most of the structures reported for this series of complexes show that the tertiary amine donor of only one of the tpa ligands is located *trans* to the μ-oxo group; in the other half of the complexes a pyridyl nitrogen atom is located *trans* to the μ-oxo group. This arrangement occurs despite the fact that the weakest donor atom of each tpa ligand, the N_{amine}, is expected to be located *trans* to the μ-oxo bridge, due to the strong *trans* influence of this bridge. The rationalization for these structures has been stereochemical; the adjacent tpa ligands are arranged more favourably in the unsymmetrical case [*i.e.* for Fe–O–Fe less than 143.4°[8d]] compared to the symmetrical arrangement, in which there may be unfavourable interligand steric interactions between the pyridine rings if both tpa N_{amine} groups are co-ordinated *trans* to the oxo bridge. Such potential steric repulsions are apparently allayed if one 2-pyridylmethyl side-arm of the tpa is replaced by a propionato group, as in the bpp complexes reported here. The symmetrical structure of **2** (both bpp N_{amine} groups *trans* to the μ-oxo) can be contrasted to the structure of its unsymmetrical tpa analogue, $[\{Fe(tpa)\}_2(MeCO_2)O][ClO_4]_3$, in which one tpa N_{amine} group is *trans* to the μ-oxo, the other *cis*.[8c] The structure of **1**, again with both bpp N_{amine} groups *trans* to the μ-oxo, can be contrasted with the structure of the only monobridged diiron complex of tpa, $[\{Fe(tpa)Cl\}_2O][ClO_4]_2$,[18] in which both tpa N_{amine} groups are *cis* to the μ-oxo group and *trans* to the terminal chloro ligands. The unfavourable interligand interactions are removed also in the complexes of (*o*-hydroxybenzyl)bis(2-pyridylmethyl)amine (hdp) (in which one 2-pyridylmethyl side-arm of the tpa has been replaced by a methylphenolato group); $[\{Fe(hdp)\}_2(PhCO_2)O][BPh_4]$ displays a symmetrical structure.[8a]

It is noteworthy to compare the diiron complexes of bpp reported here with the structures of metal complexes of related unsubstituted amino acids. The β-alaninato moiety in the structure of bis(β-alaninato)copper(II) tetrahydrate is co-ordinated in a bidentate fashion through the amine nitrogen and one carboxylate oxygen atom; the second carboxylate oxygen atom is co-ordinated to the copper centre in an adjacent molecule.[19] Thus, the aforementioned carboxylate group is capable of bridging between two metal centres, whilst the β-nitrogen atom remains attached to one of these metal ions. This situation is related to the structure represented by **I**. The arrangement of the β-alanine in its copper(II) complex can be contrasted to the arrangement of next amino acid homologue, γ-aminobutyric acid, in its copper(II) complex.[20] Here the amine

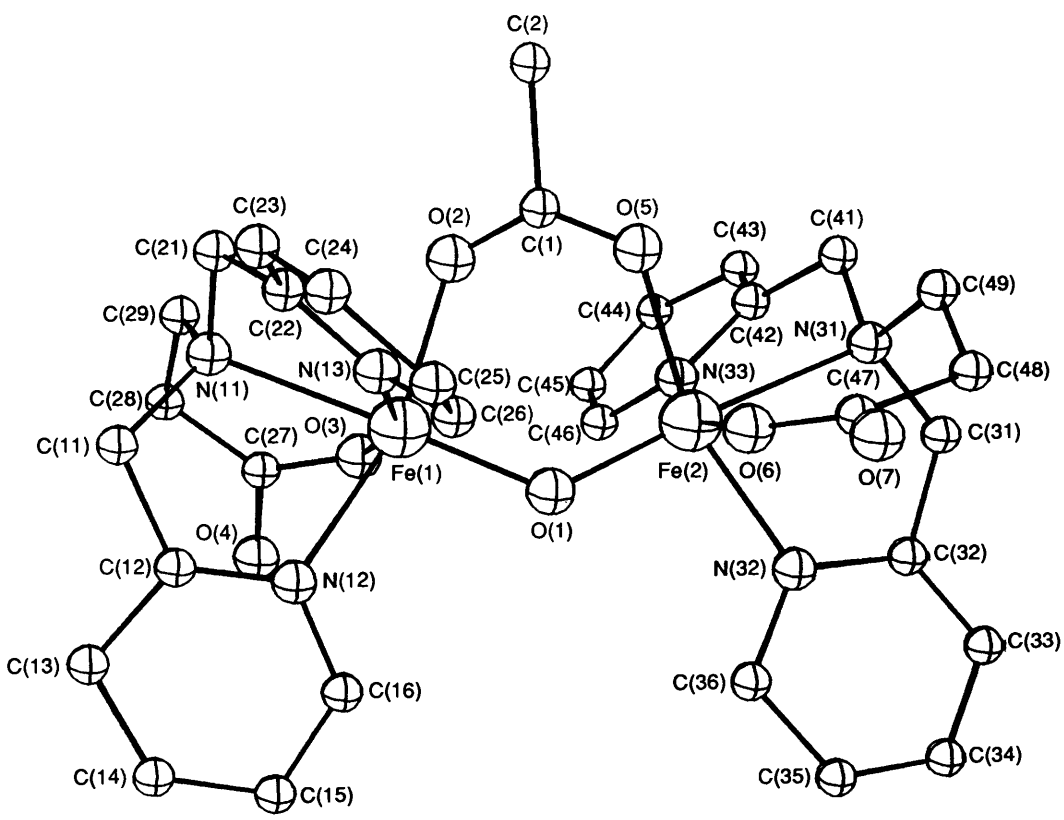

Fig. 2 The atomic arrangement for $[\{Fe(bpp)\}_2(MeCO_2)O]^+$ (cation 2) of **2** together with the numbering scheme used for both cations

Table 6 Selected bond distances (Å) and angles (°) for the two independent cations of $[\{Fe(bpp)\}_2(MeCO_2)O][ClO_4]\cdot 4.5H_2O$ **2**

	Cation 1	Cation 2
Fe(1)···Fe(2)	3.241(7)	3.249(9)
Fe(1)–O(1)	1.82(2)	1.83(2)
Fe(2)–O(1)	1.77(2)	1.77(2)
Fe(1)–O(2)	2.03(2)	2.07(2)
Fe(2)–O(5)	2.05(2)	2.05(2)
Fe(1)–O(3)	1.98(3)	1.97(3)
Fe(2)–O(6)	1.96(3)	1.97(3)
Fe(1)–N(11)	2.29(3)	2.26(3)
Fe(2)–N(31)	2.27(3)	2.29(3)
Fe(1)–N(12)	2.17(2)	2.15(3)
Fe(1)–N(13)	2.16(3)	2.14(3)
Fe(2)–N(32)	2.17(3)	2.10(3)
Fe(2)–N(33)	2.14(3)	2.23(3)
Fe(1)–O(1)–Fe(2)	129.1(10)	129.2(11)
O(1)–Fe(1)–O(2)	100.0(8)	97.2(10)
O(1)–Fe(1)–O(3)	101.7(10)	102.7(11)
O(1)–Fe(1)–N(11)	168.4(11)	172.8(12)
O(1)–Fe(1)–N(12)	97.1(10)	98.9(10)
O(1)–Fe(1)–N(13)	96.9(11)	98.0(11)
O(2)–Fe(1)–O(3)	89.2(9)	93.1(10)
O(2)–Fe(1)–N(11)	85.4(9)	85.5(10)
O(2)–Fe(1)–N(12)	162.9(10)	163.5(11)
O(2)–Fe(1)–N(13)	88.7(9)	86.6(10)
O(3)–Fe(1)–N(11)	88.6(11)	83.7(12)
O(3)–Fe(1)–N(12)	86.2(9)	86.4(11)
O(3)–Fe(1)–N(13)	161.4(12)	159.2(12)
N(11)–Fe(1)–N(12)	78.0(11)	75.6(12)
N(11)–Fe(1)–N(13)	72.8(13)	78.1(11)
N(12)–Fe(1)–N(13)	90.5(9)	88.1(10)
O(1)–Fe(2)–O(5)	100.8(9)	99.8(9)
O(1)–Fe(2)–O(6)	101.7(10)	100.7(11)
O(1)–Fe(2)–N(31)	167.2(9)	168.4(11)
O(1)–Fe(2)–N(32)	95.7(10)	97.4(10)
O(1)–Fe(2)–N(33)	98.1(10)	96.5(11)
O(5)–Fe(2)–O(6)	91.6(9)	88.2(9)
O(5)–Fe(2)–N(31)	87.9(9)	85.2(10)
O(5)–Fe(2)–N(32)	163.4(10)	162.8(10)
O(5)–Fe(2)–N(33)	85.7(9)	85.3(9)
O(6)–Fe(2)–N(31)	87.4(11)	89.8(11)
O(6)–Fe(2)–N(32)	87.2(10)	89.1(11)
O(6)–Fe(2)–N(33)	160.2(11)	162.4(11)
N(31)–Fe(2)–N(32)	75.5(10)	73.4(11)
N(31)–Fe(2)–N(33)	72.9(10)	77.8(11)
N(32)–Fe(2)–N(33)	89.9(10)	92.3(11)

nitrogen atom of one end of the amino acid is co-ordinated to one copper atom; at the other end of the ligand, the carboxylate group functions as a bidentate chelate to an adjacent copper atom. These pairs of copper atoms are *trans*-doubly bridged by γ-aminobutyrate to form an infinite one-dimensional chain in the solid state. A copper complex of the 2-pyridylmethyl-substituted γ-aminobutyric acid, in fact, the next homologue to Hbpp, 4-[bis(2-pyridylmethyl)amino]butyric acid, has been very recently reported.[21] This complex shows a structure related to its unsubstituted derivative where the pyridyl and amine nitrogen donors are co-ordinated to one copper atom and the four-carbon carboxylate 'tail' is co-ordinated to an adjacent copper atom. The unit repeats itself to form an extended chain in the solid state. These facts point to the feasibility of the carboxylate group of a β-alaninate moiety which is incorporated into a terminal capping ligand, as represented by **I** ($x = 2$), functioning as a bidentate μ-*O*,*O*′-bridging group.

The arrangement of the β-alaninate moiety of bpp in the diiron complexes reported here is not surprising in view of the six-membered chelate rings this group is capable of forming. However, the reported structures of the copper(II) complexes of unsubstituted β-alanine indicate that the desired arrangement, depicted by **I**, may be achievable, possibly without the μ-oxo ligand, and we will continue our pursuit of these complexes.

Drüeke *et al.*[22] have proposed recently an aquahydroxodiiron intermediate in their kinetic studies of the replacement of bridging acetate for a bridging phosphate. The usefulness of the diaqua complex **1**, in ligand substitution reactions, support this proposal. These substitution reactions may model, for example, the binding of phosphates to uteroferrin or the purple acid phosphatases, in which the replacement of labile water ligands may be an integral step in these catalytic processes.

Acknowledgements

A. H. is indebted to the Carlsberg Foundation and to the Danish Science Research Council for the diffractometer. This work is supported by grants from the Danish Research Council (11-9227 to H. T. and C. J. M. and 11-7916-2 to K. B. J.). We wish to thank Hanne Christensen and P. Waage Jensen for assistance with the resonance Raman measurements, Jørgen Glerup for help with the ESR measurements and Solveig Kallesøe for collecting the susceptibility data.

References

1 D. M. Kurtz, jun., *Chem. Rev.*, 1990, **90**, 585; S. J. Lippard, *Angew. Chem., Int. Ed. Engl.*, 1988, **27**, 344.
2 L. Que, jun., and A. E. True, *Prog. Inorg. Chem.*, 1990, **38**, 97.
3 N. Kitajima, N. Tamura, M. Tanaka and Y. Moro-oka, *Inorg. Chem.*, 1992, **31**, 3342; P. Chaudhuri and K. Wieghardt, *Angew. Chem., Int. Ed. Engl.*, 1985, **24**, 778; J. R. Hartman, R. L. Rardin, P. Chaudhuri, K. Pohl, K. Wieghardt, B. Nuber, J. Weiss, G. C. Papaefthymiou, R. B. Frankel and S. J. Lippard, *J. Am. Chem. Soc.*, 1987, **109**, 7387; W. B. Tolman, A. Bino and S. J. Lippard, *J. Am. Chem. Soc.*, 1989, **111**, 8522; W. B. Tolman, S. Liu, J. D. Bentsen and S. J. Lippard, *J. Am. Chem. Soc.*, 1991, **113**, 152; S. Ménage, B. A. Brennan, C. Juarez-Garcia, E. Münck and L. Que, jun., *J. Am. Chem. Soc.*, 1990, **112**, 6423; S. Ménage, Z. Yang, M. P. Hendrich and L. Que, jun., *J. Am. Chem. Soc.*, 1992, **114**, 7786; K. S. Hagen and R. Lachicotte, *J. Am. Chem. Soc.*, 1992, **114**, 8741.
4 W. H. Armstrong, A. Spool, G. C. Papaefthymiou, R. B. Frankel and S. J. Lippard, *J. Am. Chem. Soc.*, 1984, **106**, 3653.
5 B. A. Brennan, Q. Chen, C. Juarez-Garcia, A. E. True, C. J. O'Connor and L. Que, jun., *Inorg. Chem.*, 1991, **30**, 1937.
6 R. H. Beer, W. B. Tolman, S. G. Bott and S. J. Lippard, *Inorg. Chem.*, 1991, **30**, 2082.
7 D. K. Towle, C. A. Botsford and D. J. Hodgson, *Inorg. Chim. Acta*, 1988, **141**, 167; B. G. Gafford, R. A. Holwerda, H. J. Schugar and J. A. Potenza, *Inorg. Chem.*, 1988, **27**, 1126; B. G. Gafford and R. A. Holwerda, *Inorg. Chem.*, 1989, **28**, 60; H. Toftlund, S. Larsen and K. Murray, *Inorg. Chem.*, 1991, **30**, 3964; D. J. Hodgson, M. H. Zietlow, E. Pedersen and H. Toftlund, *Inorg. Chim. Acta*, 1988, **149**, 111.
8 (*a*) S. Yan, L. Que, jun., L. F. Taylor and O. P. Anderson, *J. Am. Chem. Soc.*, 1988, **110**, 5222; (*b*) S. Yan, D. D. Cox, L. L. Pearce, C. Juarez-Garcia, L. Que, jun., J. H. Zhang and C. J. O'Connor, *Inorg. Chem.*, 1989, **28**, 2509; (*c*) R. E. Norman, S. Yan, L. Que, jun., G. Backes, J. Ling, J. Sanders-Loehr, J. H. Zhang and C. J. O'Connor, *J. Am. Chem. Soc.*, 1990, **112**, 1554; (*d*) R. E. Norman, R. C. Holz, S. Ménage, C. J. O'Connor, J. H. Zhang and L. Que jun., *Inorg. Chem.*, 1990, **29**, 4629; (*e*) S. Ménage and L. Que, jun., *Inorg. Chem.*, 1990, **29**, 4293; (*f*) S. Ménage, Y. Zang, M. P. Hendrich and L. Que, jun., *J. Am. Chem. Soc.*, 1992, **114**, 7786.
9 P. Nordlund, B.-M. Sjöberg and H. Eklund, *Nature (London)*, 1990, **345**, 593.
10 E. Pedersen, *Acta Chem. Scand.*, 1972, **26**, 333; J. Josephsen and E. Pedersen, *Inorg. Chem.*, 1977, **16**, 2534.
11 C. J. O'Connor, *Prog. Inorg. Chem.*, 1982, **29**, 203.
12 G. M. Sheldrick, SHELX 86, Program for the Solution of Crystal Structures, University of Göttingen, 1986.
13 W. R. Busing, K. O. Martin and H. A. Levy, ORFLS, Report ORNL-TM-305, Oak Ridge National Laboratory, TN, 1962.
14 S. Ménage and L. Que, jun., *New J. Chem.*, 1992, **15**, 431.
15 L. Petersson, A. Gräslund, A. Ehrenberg, B.-M. Sjöberg and P. Reichard, *J. Biol. Chem.*, 1980, **255**, 6706.
16 J. Sanders-Loehr, W. D. Wheeler, A. K. Shiemke, B. A. Averill and T. M. Loehr, *J. Am. Chem. Soc.*, 1989, **111**, 8084.
17 B.-M. Sjöberg, J. Sanders-Loehr and T. M. Loehr, *Biochemistry*, 1987, **26**, 4242.

18 A. Hazell, K. Jensen, C. J. McKenzie and H. Toftlund, unpublished work.
19 Y. Mitsui, Y. Iitaka and H. Sakaguchi, *Acta Crystallogr., Sect. B*, 1976, **32**, 1634.
20 A. Takenaka, E. Oshima, S. Yamada and T. Watanabe, *Acta Crystallogr., Sect. B*, 1973, **29**, 503.
21 D. M. Stearns, L. R. Hoffman and W. H. Armstrong, *Acta Crystallogr., Sect. C*, 1992, **48**, 253.
22 S. Drüeke, K. Wieghardt, B. Nuber, J. Weiss, H.-P. Fleischhauer, S. Gehring and W. Haase, *J. Am. Chem. Soc.*, 1989, **111**, 8622.

Received 7th April 1993; *Paper* 3/02023A